American Mineralogist, Volume 84, pages 282–287, 1999

Effect of isovalent Si,Ti substitution on the bulk moduli of $Ca(Ti_{1-x}Si_x)SiO_5$ titanites

Ross J. Angel,[1,*] Martin Kunz,[2,†] Ronald Miletich,[1] Alan B. Woodland,[3] Mario Koch,[3] and Ruth L. Knoche[4]

[1]Bayerisches Geoinstitut, Universität Bayreuth, D-95440 Bayreuth, Germany
[2]High-Pressure Group, ESRF, Avenue des Martyrs, F-38043 Grenoble, France
[3]Mineralogisches Institut der Universität Heidelberg, Im Neuenheimer Feld 236, D-69120 Heidelberg, Germany
[4]Institut für Mineralogie und Petrographie, Universität Innsbruck, Innrain 52, A-6020 Innsbruck, Austria

Abstract

The equations of state of *A*2/*a* titanite phases of $CaTiSiO_5$, $Ca(Ti_{0.5}Si_{0.5})SiO_5$, and $CaSi_2O_5$ have been determined from high-pressure X-ray diffraction measurements. The isothermal bulk moduli are $K_{0,T}$ = 131.4(7) GPa (for $P > 3.6$ GPa), 151.9(1.6) GPa, and 178.2(7) GPa, respectively, for a second order Birch-Murnaghan equation-of-state (i.e., with $K' = \partial K/\partial P = 4$). Refinements of third order equations-of-state yielded values of K' that did not differ significantly from 4. The complete substitution of Si for Ti in the octahedral sites of the titanite structure, therefore, results in approximately a 30% increase in bulk modulus and a 13% increase in density. The large stiffening of the structure can be attributed to the absence of rigid-unit modes from the structure and the direct involvement of cation-cation interactions in the compression of the structure.

Introduction

Isovalent substitutions of octahedral cations in minerals usually have a relatively small effect on the bulk moduli. Examples include olivines in which the change in K_0 from Mg_2SiO_4 to Fe_2SiO_4 amounts to 4% (Isaak et al. 1989, 1993) and orthopyroxenes in which the bulk modulus changes by 8% from $MgSiO_3$ to $FeSiO_3$ (Weidner et al. 1978; Bass and Weidner 1984; Hugh-Jones and Angel 1997). However, the effect of similar isovalent substitution mechanisms involving octahedral silicon—which might be important at mantle pressures and especially in perovskites of the lower mantle—have been hampered by lack of samples. Existing data on the effect of the exchange of Si and Ti in $Ca(Ti,Si)O_3$ perovskites suggest that in this case, despite the presence of structural phase transitions, the change in bulk modulus for complete exchange of Si for Ti is around 20% (Sinelnikov et al. 1998). The recent discovery of a titanite-structured phase of $CaSiSiO_5$ (Angel 1997) and a complete solid solution between it and titanite, $CaTiSiO_5$, at high temperatures and pressures (Knoche et al. 1998) provides another opportunity to examine the effect of an Si for Ti exchange on the elasticity of solids. Therefore, the equations of state of the two end-members and one intermediate composition of this solid solution have been measured by a combination of high-pressure, single-crystal, and powder diffraction.

Experimental methods

Both the single-crystal and the powder diffraction measurements were performed with BGI design diamond-anvil cells (Allan et al. 1996) using T301 steel gaskets and a 4:1 mixture of methanol:ethanol as pressure medium. Measurements on the $CaSi_2O_5$ composition were performed with the same single-crystal used for the original determination of both the room-pressure triclinic structure (Angel et al. 1996) and the monoclinic structure (Angel 1997). A ruby chip for approximate pressure measurement and a quartz crystal as an internal diffraction pressure standard were also loaded into the pressure cell. Diffraction experiments were performed on a Huber four-circle diffractometer. Full details of the instrument and the peak-centering algorithms are provided by Angel et al. (1997). The effect of crystal offsets and diffractometer aberrations were eliminated from refined peak positions by the eight-position centering method of King and Finger (1979). Unit-cell parameters determined by a least-squares fit to the corrected setting angles of reflections showed no deviations from symmetry-constrained values greater than one estimated standard deviation. The values of symmetry-constrained unit-cell parameters obtained by vector-least-squares (Ralph and Finger 1982) are reported in Table 1.

Intensity data were also collected from this crystal in the monoclinic form at room pressure in air (Angel 1997) and at four pressures in the diamond-anvil pressure cell using an Enraf-Nonius CAD4 diffractometer. Details of data collection and reduction procedures followed those described in detail in Miletich et al. (1998), among others. Refined coordinates for the *A*2/*a* structure of $CaSi_2O_5$ at high pressure are provided in Table 2 and selected bond lengths in Table 3.

At pressures in excess of 5.9 GPa the diffraction peaks

* E-mail: ross.angel@uni-bayreuth.de
† Current address: Labor für Kristallographie, ETH Zürich, Switzerland

TABLE 1. Cell parameters of $CaSi_2O_5$ at pressure obtained by single-crystal diffraction

P (GPa)	*a* (Å)	*b* (Å)	*c* (Å)	β (deg)	*V* (Å³)
0.0001	6.5430(6)*	8.3918(4)	6.3416(5)	113.175(6)	320.10(4)
0.559(9)	6.5371(10)	8.3873(4)	6.3312(5)	113.139(10)	319.21(7)
0.996(7)	6.5297(10)	8.3823(4)	6.3227(5)	113.087(10)	318.35(7)
1.955(8)	6.5176(9)	8.3710(4)	6.3065(4)	113.006(8)	316.71(6)
2.556(9)	6.5090(11)	8.3635(4)	6.2967(5)	112.953(10)	315.64(7)
2.626(10)	6.5096(10)	8.3636(4)	6.2954(5)	112.960(9)	315.59(7)
3.427(14)	6.4986(9)	8.3544(4)	6.2816(4)	112.881(8)	314.20(6)
4.333(12)	6.4871(11)	8.3449(5)	6.2679(4)	112.811(10)	312.77(7)
4.438(9)	6.4850(8)	8.3431(6)	6.2653(6)	112.784(12)	312.53(7)
4.889(13)	6.4814(9)	8.3385(4)	6.2588(4)	112.774(8)	311.89(6)
5.798(12)	6.4699(9)	8.3294(4)	6.2444(4)	112.688(9)	310.48(6)
5.90(1)†	6.4690(7)	8.3280(6)	6.2435(6)	112.681(11)	310.37(6)

* Numbers in parentheses represent 1 esd. This convention also applies to all subsequent tables.
† Pressure from ruby spectra only.

of the $CaSi_2O_5$ crystal became broadened but became sharp again on reducing the pressure in the diamond-anvil cell. This behavior was repeated both on a further pressurization cycle with this crystal and with other crystals synthesized in a different multi-anvil run. No explanation is presented here for the cause of this reflection broadening, although some possibilities can be excluded. For instance, non-hydrostaticity of the pressure media is not the cause, because the methanol:ethanol mixture remains hydrostatic to pressures of ~10 GPa (Piermarini et al. 1973) and the quartz crystals mounted in the same cell exhibited no peak broadening at all. Also excluded is bridging of the crystal between the diamond anvils because in some of the mounts the sample crystal was thinner than the quartz crystal. Whether this broadening, therefore, reflects a further structural phase transition, incipient amorphization, or some other process must await further investigations.

Powder diffraction measurements were performed on samples of $CaTiSiO_5$ composition and nominally $Ca(Ti_{0.5}Si_{0.5})SiO_5$ composition. The synthesis and characterization of the $CaTiSiO_5$ sample (designated 96–1), is described in full by Xirouchakis et al. (1997a, 1997b). The sample of nominal 50:50 composition is a portion of the single-phase products from run H567 described by Knoche et al. (1998), a multi-anvil synthesis conducted at 8.5 GPa and 1350 °C. Microprobe analysis of the run product gave a composition of $Ca_{0.97(1)}Ti_{0.52(2)}Si_{1.50(2)}O_5$. These two samples were separately mixed with quartz powder to act as an internal high-pressure diffraction standard and a few chips of ruby for approximate pressure measurement. High-pressure powder diffraction patterns were collected at beamline ID30 at the ESRF, Grenoble, using an incident beam wavelength of 0.5134 Å (as determined from a diffraction pattern of Si standard material) and an image plate located approximately 29.5 cm from the sample position. Image plate data were corrected and calibrated by the procedures of Hammersley et al. (1995) and integrated to conventional constant-step-size intensity-2θ patterns using the Fit2d software (Hammersley 1997; Hammersley et al. 1996). Full-pattern Le-Bail refinements (Le Bail 1992) were then performed with the GSAS program package (Larsen and von Dreele 1988) to yield cell parameters for the samples and the quartz (Table 4). The unit-cell data for $CaTiSiO_5$ were presented by Angel et al. (1998) who analyzed the high-pressure $P2_1/a$ to $A2/a$ phase transition that occurs in this sample at ~3.6 GPa.

Equation-of-state parameters of all three samples were obtained by a weighted-least-squares fit of the Birch-Murnahan third order equation-of-state (EOS) (Birch 1947) to the pressure-volume data. Pressures were determined from the unit-cell volumes of the quartz included in the diamond-anvil cell using the equation-of-state reported by Angel et al. (1997). Weights in the refinement were calculated from the estimated standard deviations (esd) of

TABLE 2. Refined coordinates for $CaSi_2O_5$ at high pressures from single-crystal X-ray diffraction

Site	Coordinate	1 atm*	1.0 GPa	2.6 GPa	4.4 GPa	5.8 GPa
Ca	*y*	0.42059(9)	0.4202(2)	0.4197(5)	0.4194(5)	0.4191(3)
Si^{IV}	*y*	0.43657(13)	0.4361(3)	0.4378(7)	0.4378(7)	0.4369(4)
O1	*y*	0.3090(4)	0.3098(8)	0.3108(14)	0.3115(17)	0.3098(10)
O2	*x*	0.9142(3)	0.9201(3)	0.915(4)	0.928(4)	0.916(3)
O2	*y*	0.3178(2)	0.3184(6)	0.3178(10)	0.3191(11)	0.3194(6)
O2	*z*	0.4477(3)	0.4481(11)	0.4461(22)	0.4475(19)	0.4446(15)
O3	*x*	0.3958(3)	0.3985(3)	0.408(6)	0.396(4)	0.393(3)
O3	*y*	0.4500(2)	0.4497(6)	0.4510(10)	0.4507(13)	0.4497(7)
O3	*z*	0.6531(3)	0.6547(11)	0.655(3)	0.6514(19)	0.6487(13)

Notes: Positions for the atoms are ¼, *y*, ¼ for Ca; ½, ¼, ¾ for Si^{VI}; ¾, *y*, ¼ for Si^{IV}; ¾, *y*, ¾ for O1; and *x, y, z* for O2 and O3.
* Data taken from Angel (1997).

TABLE 3. Selected bond lengths (Å) for $CaSi_2O_5$ at pressure from single-crystal diffraction.

		1 atm*	1.0 GPa	2.6 GPa	4.4 GPa	5.8 GPa
Ca-O1	[1]†	2.269(3)†	2.262(7)	2.254(12)	2.246(14)	2.258(8)
Ca-O2	[2]	2.381(2)	2.390(7)	2.364(13)	2.388(13)	2.359(9)
Ca-O3	[2]	2.364(2)	2.367(6)	2.360(16)	2.330(11)	2.311(7)
Ca-O3	[2]	2.410(2)	2.395(12)	2.336(30)	2.393(21)	2.408(14)
Avg.		2.368	2.367	2.339	2.353	2.345
Si^{6+}-O1	[2]	1.709(1)	1.708(2)	1.705(4)	1.701(4)	1.692(2)
Si^{6+}-O2	[2]	1.862(2)	1.861(6)	1.860(11)	1.858(9)	1.862(8)
Si^{6+}-O3	[2]	1.824(2)	1.814(7)	1.807(13)	1.821(12)	1.818(7)
Avg.		1.798	1.794	1.791	1.793	1.791
Si^{6+}-O2	[2]	1.631(2)	1.639(9)	1.628(17)	1.651(15)	1.605(11)
Si^{6+}-O3	[2]	1.629(2)	1.637(8)	1.661(21)	1.611(15)	1.613(10)
Avg.		1.630	1.638	1.645	1.631	1.609

* Data from Angel (1997).
† Numbers in square brackets indicate bond multiplicities.
‡ Incorrectly given as 2.229 Å in Angel (1997).

the unit-cell volumes of the titanites combined with the uncertainty in pressure corresponding to the esd of the unit-cell volumes of the quartz pressure standard. Strain tensors were calculated for each pressure from the unit-cell parameters at pressure using those measured at room pressure as the reference basis.

RESULTS

Unit cells of the monoclinic polymorph of $CaSi_2O_5$ were determined at room pressure and at 11 pressures to a maximum of 5.9 GPa. The least-squares fit of the volume-pressure data yield for the Birch-Murnahan finite strain EOS the values $V_0 = 320.12(2)$ Å^3, $K_{0,T} = 178.2(7)$ GPa with K' fixed at 4. Refinement of K' resulted in a value of 4.9(8) with no significant reduction in χ^2_w of the fit. We therefore conclude that the second-order Birch-Murnahan EOS (i.e., with $K' = 4$) is an adequate description of the compression of $CaSi_2O_5$ (Fig. 1). The maximum residual $P_{obs} - P_{calc}$ in this fit is 0.046 GPa and $\chi^2_w = 0.42$.

The $Ca(Ti,Si)SiO_5$ sample has $A2/a$ symmetry at room pressure and temperature (Knoche et al. 1998), and all diffraction patterns collected to a maximum pressure of 7.39 GPa indicated that the symmetry remains unchanged. Refinement of the third order Birch-Murnahan EOS yielded $K' = 5.6(1.8)$, again indicating that it does not differ significantly from the value of $K' = 4$. With this constraint, we obtain a value of 151.9(1.6) GPa for the zero-pressure bulk modulus (Fig. 1) with $P_{obs} - P_{calc\ max} = 0.09$ GPa and $\chi^2_w = 13.3$ for 10 data.

End-member $CaTiSiO_5$ has space group symmetry $P2_1/a$

TABLE 4. Cell parameters of $Ca(Ti_{0.5}Si_{0.5})SiO_5$ at pressure obtained by powder diffraction

P (GPa)	a (Å)	b (Å)	c (Å)	β (deg)	V (Å^3)
0.000(5)	6.7877(3)	8.5458(4)	6.4563(3)	113.659(3)	343.03(4)
1.048(5)	6.7715(3)	8.5348(3)	6.4347(2)	113.528(2)	340.96(3)
1.835(5)	6.7570(3)	8.5222(3)	6.4176(3)	113.462(3)	339.00(3)
2.855(7)	6.7416(3)	8.5092(3)	6.3977(3)	113.383(3)	336.87(3)
3.661(9)	6.7277(4)	8.5009(4)	6.3814(4)	113.283(3)	335.24(5)
4.629(8)	6.7121(3)	8.4868(3)	6.3638(3)	113.234(3)	333.11(3)
5.391(10)	6.7023(4)	8.4798(4)	6.3504(4)	113.142(4)	331.88(4)
6.144(11)	6.6902(4)	8.4696(5)	6.3373(4)	113.092(4)	330.32(5)
6.909(10)	6.6810(3)	8.4626(4)	6.3260(4)	113.032(4)	329.15(4)
7.387(10)	6.6745(3)	8.4562(4)	6.3176(4)	112.999(4)	328.23(4)

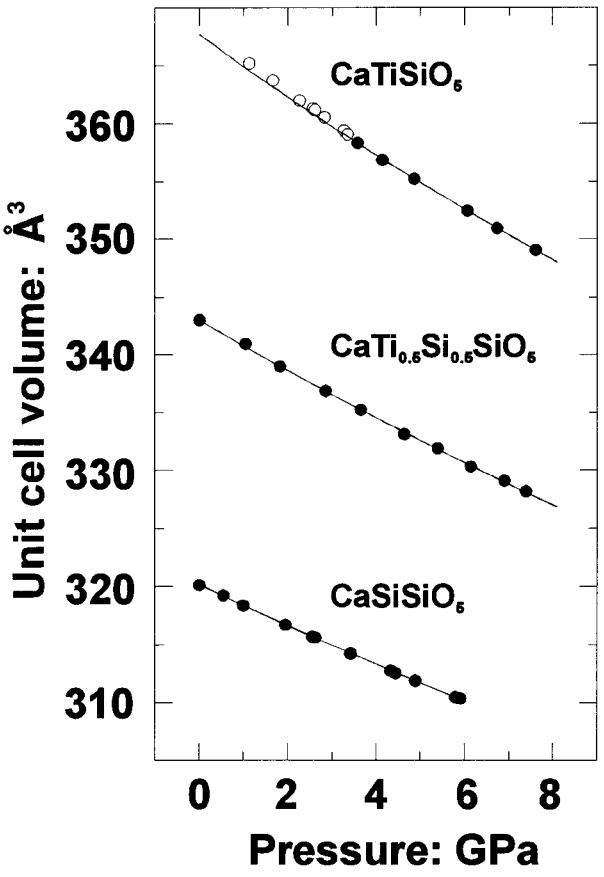

FIGURE 1. Volume-pressure data for the three titanite phases. The open symbols are data for the $P2_1/a$ phase of the $CaTiSiO_5$ sample and were not included in the fit of the equation-of-state to the high-pressure $A2/a$ phase. Solid lines are the Birch-Murnahan second-order equation-of-state fit to the volume-pressure data.

at room temperature and pressure as a result of ordering of the displacements of Ti atoms from the centers of the TiO_6 octahedra. Kunz et al. (1996) found that at a P = 6.2 GPa titanite has the aristotype structure with $A2/a$ symmetry. The pressure of the $P2_1/a$ to $A2/a$ phase transition has subsequently been determined to be ~3.6 GPa (Angel et al. 1998). Refinement of a Birch-Murnahan EOS to the volume-pressure data for the two phases fitted separately with K' constrained to 4 yields $K_{0,T}$ = 123.3(1.2) GPa for the low-pressure phase (8 data) and $K_{0,T}$ = 131.4(7) GPa for the 6 data in the high-pressure phase (Fig. 1). Maximum residuals are $P_{obs} - P_{calc\ max}$ = 0.03 and 0.02 GPa and χ^2_w = 19 and 6.7 for the low- and high-pressure phases respectively. Refinements of K' yield values do not differ significantly from 4 within the large uncertainties.

The unit-cell parameters of all three samples exhibit very similar behavior with the major change being the decrease in the β unit-cell angle with increasing pressure (Tables 1 and 4; Angel et al. 1998). The strain tensors (Nye 1958) that describe the compression represent the same constant orientation of the strain ellipsoid in $CaSi_2O_5$ and the 50:50 composition. In both samples the intermediate principal axis of compression is parallel to the b axis of the unit cell. The softest principal axis lies in the (010) plane, 19 ± 3° away from the c axis toward the $[\bar{1}00]$ direction. The stiffest axis is perpendicular to these two, also lying in the (010) plane (Fig. 2), close to the [403] direction. In $CaSi_2O_5$, the compression along the two stiffer principal axes differs by ~10%, whereas in the 50:50 composition, they are equal within the uncertainties. This trend is continued to titanite itself in which the stiffest principal axis is parallel to the b axis of the unit cell. In addition, $CaTiSiO_5$ differs in that the softest principal axis is rotated further (39 ± 2°) away from $+c$ toward [−100]. Despite these differences, between 50 and 60% of the volume compression of all three samples occurs along this softest direction.

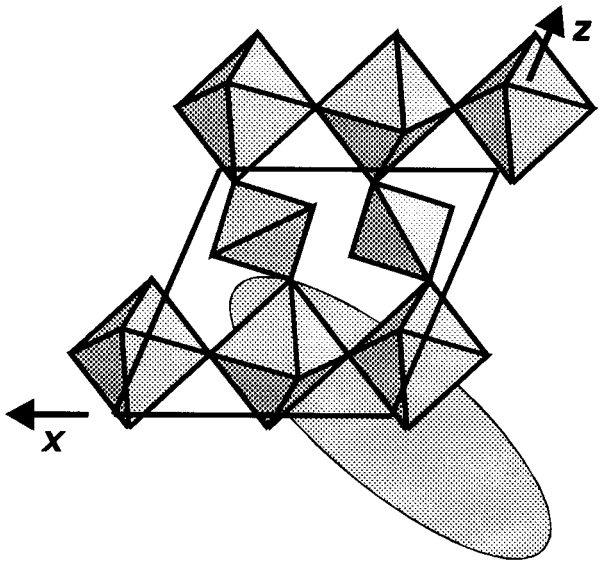

FIGURE 2. A portion of the polyhedral framework of the $A2/a$ titanite aristotype structure, emphasizing the six-membered rings comprised of tetrahedra and octahedra that appear to be responsible for the large shear in (010) that occurs under compression. The ellipse represents the orientation and anisotropy of the (010) section of the strain ellipsoid that describes the behavior of the Unit cell of $CaSi_2O_5$ upon compression.

DISCUSSION

Anisotropy

High-compressional anisotropy is usually attributed to either a layering of the crystal structure as in micas (Hazen and Finger 1978) or to the ability of the structure to compress through the relative rotation of stiff corner-linked polyhedra, as occurs in the feldspars that uniformly display 60% anisotropy in compression (Angel 1994). Neither of these causes are applicable to titanite. Nor does the apparent high degree of anisotropy result from strong anisotropy in atomic compression mechanisms within the structure but results directly from the reduction with pressure of the β unit-cell angle. If β is reduced without any change in the unit-cell edges, the [101] direction would be within 1° of the direction of maximum extension and $[10\bar{1}]$ close to the direction of maximum compression. For $CaSi_2O_5$, the reduction of β from 113.18° at room pressure to 112.69° at 5.8 GPa would alone result in changes in length of these directions of 0.65 Å, if the unit-cell edges remained constant. This change amounts to linear strains of +0.0064 for [101] and −0.0028 for $[10\bar{1}]$ arising from the shear alone. The observed high anisotropy of compression in the (010) plane (Fig. 2) arises, therefore, from the addition of this shear contribution to an overall isotropic linear compression of −0.013, yielding the observed linear strains of −0.007 for [101] and −0.016 for $[10\bar{1}]$.

The structural origin of the compressional anisotropy can be attributed to the arrangement of the more compressible CaO_7 polyhedra within the structure. These polyhedra form chains parallel to [101], and the chains are cross-linked through shared edges with the octahedra. Therefore, it is not unreasonable to find that the b axis, which is perpendicular to these CaO_7 chains, is the stiffest direction in the structure. The structural origin of the shear, or reduction in the β angle with pressure, is in the shearing of one of the larger polyhedral rings within the structure (Fig. 2), presumably induced as a result of competition between the compression of the CaO_7 chains and the polyhedral framework. The positions of the six cations forming this ring remain invariant with pressure relative to the unit-cell in $CaSi_2O_5$ (Table 2), so this ring as a whole must undergo shear. Unfortunately, because the shear is distributed over many bond angles, the changes are not discernible in the results of the high-pressure structure refinements of $CaSi_2O_5$.

Bulk modulus

The complete substitution of silicon for titanium on the octahedral site of the titanite structure results in a ~30% stiffening of the structure, whereas the unit-cell volume decreases by only ~13% from titanite to $CaSi_2O_5$. Both trends are linear in composition (see Knoche et al. 1998, for additional volume data) indicating that the phase transitions are not an influence on these trends. The observed stiffening is, therefore, larger than expected from the relationship KV_0 = constant, which was derived from simple considerations and proposed by Shankland (1972), among others. The stiffening can, however, be understood on the basis of the topology of the polyhedral framework of the titanite structure type. This framework possesses no rigid-unit modes (Hammonds et al. 1998). Therefore, the structure cannot reduce volume by polyhedral rotation alone, but compression must involve compression and deformation of either the tetrahedra or the octahedra or both. For these reasons, any change in volume of the titanite structure has to be produced by shortening of bonds. The observed compressibility in titanite is thus directly related to the bond-strengths in the same way that in such cases vibrational frequencies directly depend on bond strengths (e.g., Hofmeister 1991).

Furthermore, the octahedral cations are constrained to lie on the centers of symmetry in the *A*2/*a* structure, and M-M distances along the octahedral chains must by symmetry follow the compression of the *a*-cell edge. In addition, the silicon tetrahedral position has only one variable coordinate, *y*. This does not vary with pressure in the $CaSi_2O_5$ end-member (Table 2). Thus, the octahedral and tetrahedral cations form an array that only deforms along with the unit cell. Therefore, direct cation-cation repulsion between these cations as a primary control on compression of the structure can be expected. The 8% reduction in octahedral-octahedral cation distance in going from $CaTiSiO_5$ (Ti-Ti = 3.535 Å) to $CaSi_2O_5$ (Si^{VI} – Si^{VI} = 3.272 Å) and the 4% reduction in the average T-M distances (from 3.357 to 3.214 Å) can readily account for much of the stiffening of the structure. The intrinsic rigidity of the polyhedral framework also means that the ''extra-framework'' Ca atom is intimately involved in the compression of the structure, as indicated by the compressional anisotropy. Thus, an additional contribution from the CaO_7 polyhedra to the increase in bulk modulus across the solid solution may exist because the average <Ca-O> bond length of $CaSi_2O_5$ is 4% shorter than in $CaTiSiO_5$. Thus, relative to $CaTiSiO_5$, the calcium coordination polyhedra in $CaSi_2O_5$ are ''pre-compressed'' by the smaller octahedra and are probably stiffer. Confirmation, of course, must await high-pressure structure refinements of titanite itself.

Many of the phases stable at the pressures of the Earth's transition zone have structures comprised of both silicate octahedra and tetrahedra. Hammonds et al. (1998) have noted that many structures with such mixed polyhedral networks of octahedra and tetrahedra also possess no rigid-unit modes. Therefore, if the sensitivity of the titanite structure to Si/Ti substitution is typical of that of other structures and of other substitutions for Si (because of the absence of rigid modes), then enhanced sensitivity of elastic properties to composition in several phases present in the transition zone of the Earth can be expected. By contrast to these and similar to the lower-pressure tetrahedral framework structures, perovskites possess many rigid-unit modes and hence a weaker sensitivity of elastic properties to isovalent cation substitution as recently demonstrated by Sinelnikov et al. (1998).

Acknowledgments

Dimitrios Xirouchakos kindly donated the $CaTiSiO_5$ sample used in these experiments. Stany Bauchau and Michael Hanfland are thanked for assistance and advice during the powder diffraction experiments at ESRF. Bob Liebermann and Martin Dove kindly provided relevant manuscripts prior to their publication.

References cited

Allan, D.R., Miletich, R., and Angel, R.J. (1996) A diamond-anvil cell for single-crystal X-ray diffraction studies to pressures in excess of 10 GPa. Reviews of Scientific Instruments, 67, 840–842.

Angel, R.J. (1994) Feldspars at high pressure. In I. Parsons, Ed., Feldspars and their reactions, p. 271–312. Kluwer, Dordrecht, The Netherlands.

——— (1997) Transformation of fivefold-coordinated silicon to octahedral silicon in calcium silicate, $CaSi_2O_5$. American Mineralogist, 82, 836–839.

Angel, R.J., Ross, N.L., Seifert, F., and Fliervoet, T.F. (1996) Structural characterization of pentacoordinate silicon in a calcium silicate. Nature, 384, 441–444.

Angel, R.J., Allan, D.R., Miletich, R., and Finger, L.W. (1997) The use of quartz as an internal pressure standard in high-pressure crystallography. Journal of Applied Crystallography, 30, 461–466.

Angel, R.J., Kunz, M., Miletich, R., Woodland, A.B., Koch, M., and Xirouchakis, D. (1998) High-pressure phase transition in $CaTiOSiO_4$ titanite. Phase Transitions, in press.

Bass, J.D. and Weidner, D.J. (1984) Elasticity of single crystal orthoferrosilite, Journal of Geophysical Research, 89, 4359–4371.

Birch, F. (1947) Finite elastic strain of cubic crystals. Physical Review 71, 809–824.

Hammersley, A.P. (1997) FIT2D: An introduction and overview. ESRF Internal Report ESRF97HA02T. ESRF, Grenoble, France.

Hammersley, A.P. Svensson, S.O., Thompson, A, Graafsma, Kvick, A., and Moy, J.P. (1995) Calibration and correction of distortions in 2D detector systems. Reviews of Scientific Instruments, 66, 2729–2733.

Hammersley, A.P., Svensson, S.O., Hanfland, M., Fitch, A.N., and Häusermann, D. (1996) Two-dimensional detector software: from real detector to idealised image or two-theta scan. High-Pressure Research, 14, 235–248.

Hammonds, K.D., Bosenick, A., Dove, M.T., and Heine, V. (1998) Rigid unit modes in crystal structures with octahedrally coordinated atoms. American Mineralogist, 83, 476–479.

Hazen, R.M. and Finger, L.W. (1978) The crystal structures and compressibilities of layer minerals at high pressure. II. Phlogopite and chlorite. American Mineralogist, 63, 293–296.

Hofmeister, A. (1991) Calculation of bulk modulus and its pressure derivatives from vibrational frequencies and mode Grüneisen parameters: solids with cubic symmetry or one nearest-neighbour distance. Journal of Geophysical Research, 96B, 16181–16203.

Hugh-Jones, D.A. and Angel, R.J. (1997) The effect of Ca^{2+} and Fe^{2+} on the equations of state and compressional behavior of $MgSiO_3$ pyroxenes. Journal of Geophysical Research, 102B, 12333–12340.

Isaak, D.G., Anderson, O.L., and Goto T. (1989) Elasticity of single-crystal forsterite measured to 1700 K. Journal Geophysical Research, 94, 5895–5906.

Isaak, D.G., Graham, E.K., Bass, J.D., and Wang, H. (1993) The elastic

properties of single-crystal fayalite as determined by dynamical measurement techniques. Pure and Applied Geophysics Letters, 141, 393–414.

King, H. and Finger, L.W. (1979) Diffracted beam crystal centring and its application to high-pressure crystallography. Journal of Applied Crystallography, 12, 374–378.

Knoche, R.L., Angel, R.J., Seifert, F., and Fliervoet, T.F. (1998) Complete substitution of Si for Ti in titanite $Ca(Ti_{1-x}Si_x)^{VI}Si^{IV}O_5$. American Mineralogist, 83, 1168–1175.

Kunz, M., Xirouchakis, D., Lindsley, D.H., and Häusermann, D. (1996) High-pressure phase transition in titanite ($CaTiOSiO_4$). American Mineralogist, 81, 1527–1530.

Larsen, A.C. and Von Dreele, R.B. (1988) General Structure Analysis System (GSAS). los Alamos National Laboratory Report LA-UR 86–748. Los Alamos, New Mexico.

Le Bail, A. (1992) Extracting structure factors from powder diffraction data by iterative full pattern profile fitting. In Prince, E. and Staljek, J.K., Eds., Accuracy in powder diffraction II, Special publication 846, p. 213. National Institute of Standards and Technology, Gaithersburg, Maryland.

Miletich, R., Seifert, F., Angel, R.J. (1998) Compression of cadmium orthosilicate Cd_2SiO_4: A high-pressure single-crystal diffraction study. Zeitschrift für Kristallographie, 213, 288–295.

Nye, J.F. (1958) Physical Properties of Crystals. Oxford University Press, Oxford, England.

Piermarini, G.J., Block, S., and Barnett, J.D. (1973) Hydrostatic limits in liquids and solids to 100 k-bar. Journal of Applied Physics, 44, 5377–5382

Ralph, R.L. and Finger, L.W. (1982) A computer program for refinement of crystal orientation matrix and lattice constants from diffractometer data with lattice symmetry constraints. Journal of Applied Crystallography, 15, 537–539.

Shankland, T.J. (1972) Velocity-density systematics: Derivation from Debye theory and the effect of ionic size. Journal Geophysical Research, 77, 3750–3758.

Sinelnikov, Y.D., Chen, G., and Liebermann, R.C. (1998) Elasticity of $CaTiO_3$-$CaSiO_3$ perovskites. Physics and Chemistry of Minerals, 25, 515–521.

Weidner, D.J., Wang, H., and Ito, J. (1978) Elasticity of orthoenstatite. Physics of the Earth and Planetary Interiors, 17, 7–13.

Xirouchakis, D., Kunz, M., Parise, J.B., and Lindsley, D.H. (1997a) Synthesis methods and unit-cell volume of end-member titanite ($CaTiOSiO_4$). American Mineralogist, 82, 748–753.

Xirouchakis, D., Fritsch, S., Putnam, R.L., Navrotsky, A. and Lindsley, D.H. (1997b) Thermochemistry and the enthalpy of formation of synthetic end-member ($CaTiSiO_5$) titanite. American Mineralogist, 82, 754–759.

Manuscript received March 31, 1998
Manuscript accepted September 30, 1998
Paper handled by Robert M. Hazen